Journal of Information Systems and Telecommunication
Vol.14, No.2, April-June 2026, 170-181
http://jist.acecr.org
ISSN 2322-1437 / EISSN:2345-2773

A Spectral-Domain Approach for Early Blockage Detection in Sub-Terahertz Wireless Networks

Neravati Nagaraja Kumar[1], Anil Kumar[2*], Subba Raju MP[3], Kalyani Kapula[4], Surya Kala Nagireddi[5], Yarrapragada Rao K. S. S[5]

[1].Department of Electronics and Communication Engineering, Rajeev Gandhi Memorial College of Engineering and Technology, Nandyal, India
[2].Department of Electronics and Communication Engineering, Aditya University, Surampalem, India
[3].Department of Electrical and Electronics Engineering, Aditya University, Surampalem, India.
[4].Department of Electronics and Communication Engineering, Aditya University, Surampalem, India.
[5].Department of Information Technology, Aditya University, Surampalem, India.
[6].Department of Mechanical Engineering, Aditya University, Surampalem, India.

Received: 31 Dec 2024/ Revised: 04 Jul 2026/ Accepted: 02 Aug 2026

Abstract

The paper presents the problem of human body blockage in sub-terahertz and millimeter wave wireless systems. These communication systems are operated at very high frequencies. The generated high frequency signals are very sensitive to obstacles like the human body. A blockage event abruptly reduces the received signal power. This causes a loss of signal connection between transmitter and receiver. To avoid this problem, the network detects a blockage before it actually happens. Many existing solutions use machine learning models in the time domain. These methods are complex. Long training times are required. The signal shows clear oscillations just before a blockage happens. These oscillations are weak in the time domain. The paper uses the short-time Fourier transform to extract spectral features from the received signal. The difference between normal conditions and pre-blockage conditions becomes very large. In some cases, the gap reaches two orders of magnitude. Based on this observation, a threshold-based proactive blockage detection algorithm is designed. The algorithm is simple and does not rely on machine learning. In order to solve this, MATLAB simulation environment is assumed with parameter values and data collected at 156~GHz in an indoor environment. The performance is measured using blockage detection probability, mean time to blockage and false alarm rate. The paper explains the spectral analysis offers a simple and effective way to enable proactive blockage detection for future sub-terahertz wireless networks.

Keywords: Sub-Terahertz Communication; Human Body Blockage; Proactive Blockage Detection; Short-Time Fourier Transform; Spectral-Domain Analysis; Threshold-Based Detection Algorithm.

1- Introduction

Millimeter wave and sub-terahertz communications are used to help in current and future wireless networks [1]. These systems are 5G enabled and are likely to form the basis of 6G network. This is operated at extremely high carrier frequencies. Normal millimeter wave frequencies are between 30 and 70 GHz[2]. Sub-terahertz range is between 100 and 300 GHz. These frequency bands are of very large bandwidth. Extremely high data rates are made possible by large bandwidth. It will be essential in such applications as virtual reality, smart factories and high-speed connectivity within the premises. But these advantages are associated with severe technical difficulties [3]. Huge obstacle is blockage of the human body. Radio wave frequencies in the millimeter and sub tehertz range cannot easily bend around objects. As soon as a human body enters the line-of-sight between the transmitter and receiver, the signal power reduces to a sharp [4].

In most occasions, it leads to total disconnection. The issue is highly prevalent in the indoor setting, because individuals relocate regularly. Consequently, human congestion will be among the greatest impediments to dependable high-frequency communication [5]. In order to make the effects of blockage lower, multiple system-level solutions were offered. Multiconnectivity is one of the solutions. This

✉ **Anil Kumar R**
anidecs@gmail.com

method enables a user device to have several parallel connections with diverse base stations. In the event of link being blocked, the traffic is redirected to another link. Multiconnectivity involves the high concentration of base stations [6]. It relies on rapid and responsive blockage detection. Another solution is integrated access and backhaul. In this approach, low-cost relay nodes are used to bring access points closer to users. This reduces the probability of line-of-sight blockage. While this method helps reduce blockage effects, it does not fully eliminate them[7]. Occasional blockages still happen. Both multiconnectivity and integrated access and backhaul require one key capability. The network needs to detect blockage events before the signal is fully blocked [8]. Proactive detection aims at the detection of an impending blockage event prior to an eventual obstruction of the signal. In case the network forecasts the blockage early, it prevents measures are taken. Such activities involve beam switching, link switching or traffic diversion[9]. These measures require time to accomplish. As such, the blockage must be identified tens of milliseconds beforehand. This renders proactive detection quite difficult compared to reactive detection. Recurrent neural networks and deep neural networks are usually employed[10]. Although these techniques are performing well, they are characterized by obvious shortcomings. Considerable amounts of training data are needed. Retraining is required when there is a change in conditions. Other methods are based on other sensing measurements. The measurements have made a significant finding: the received signal has little oscillations just before a blockage occurs[11]. In the case where a human body comes close to the line-of-sight path, partial obstruction occurs. This causes interference patterns. Such patterns are manifested in the received signal power in the form of ripples[12]. This observation is furthered in this paper and a new perspective is suggested. The paper is based on the spectral domain rather than the time domain analysis of the signal. The point is that small swings at the time domain result to strong content at the frequency domain. Through spectral analysis, the variance between normal functioning and pre-blockage is far more obvious[13].

This paper promotes short time fourier transform applied to get spectral representation of received signal. It is shown by adding short window spectral energy that pre-blockage periods have far more spectral energy than non-blockage periods[14]. The difference is in most cases two orders of magnitude. The existence of this wide gap provides the opportunity to use basic threshold-based detection techniques. Complex machine learning models are not needed. The protracted training periods are unnecessary. It is the indoor sub-terahertz deployments. Experimental records of measurements at 156 GHz are utilized[15]. This rate is very applicable to the 6G systems of the future. The measurements are realistic human blockage behaviour. This renders the evaluation a practical and reliable evaluation. This paper has made some important contributions that include:

- To present spectral-domain analysis in proactive human blockage detection in sub-terahertz communication systems. To show that separability between pre-blockage and non-blockage can occur with spectral power differences up to two orders of magnitude.
- To implement threshold-based proactive blockage detection algorithm, not based on machine learning models.
- To test the proposed method with real indoor measurement data at 156~GHz with realistic blockage conditions.
- To operate at a false alarm rate that is less than one event/second in fading environments.

The paper suggests a preventive blockage sensing algorithm based on spectral analysis. The algorithm is basic and uncomplicated. It works in various phases to deal with initializing, detecting and restoring [16]. It continuously monitors the spectral power of the received signal. When the power exceeds a defined threshold, a blockage is predicted. The algorithm is implemented at the user device or the base station [17]. Its computational complexity is low. The introduction highlights that the proposed approach overcomes the limitations of existing methods. It avoids machine learning. It does not require training. It is robust to fading and noise. It detects blockage early enough to support system-level mitigation techniques [18]. These properties make it suitable for practical sub-terahertz networks.

2- Related Work

Human body blockage received wide attention in millimeter wave and sub-terahertz wireless systems. Early measurement-based studies showed that human bodies cause very large attenuation at high frequencies. In [19], human blockage at 73~GHz was analyzed and a diffraction-based model was proposed. The results showed that blockage leads to sudden and severe signal drops. Several studies investigated empirical blockage characterization. In [20], a large-scale indoor measurement campaign was conducted at sub-terahertz frequencies. Blockage attenuation, duration and temporal characteristics were analyzed. The analysis showed that blockage events are frequent and highly dynamic in indoor environments. This work provided important measurement data that later studies used for blockage detection research. However, the focus was on reactive detection and statistical modeling, not proactive prediction. System-level solutions were suggested to reduce the effects of blockages. Multi-connectivity is one of the biggest solutions, standardized by 3GPP in Release~16 [21]. Multi-connectivity enables user equipment to have several simultaneous connections. The research that involved [22] revealed that multi-connectivity enhances continuity of a session in mmWave systems. This is because link switching is time consuming and relies on the timely detection of blockage. Multi-connectivity, in itself is not enough without proactive detection.

Integrated access and backhaul is another system-level solution. In [23], the 3GPP taskforce suggested the application of relay nodes to enhance coverage and low blockage likelihood. It was analyzed in [24] that integrated access and backhaul has the benefit of minimizing blockage effects in dense deployments. Nevertheless, this is based on rapid blockage sense. It is not able to completely reduce the blockage events. Early warning is a very important necessity. The majority of the methods of early blockage detection were reactive. These techniques only identify when blockage has occurred when the signal received falls below a threshold. These methods are not complex yet cannot be used in smooth communication. The signal is lost and often it is already too late to avoid the interruption of the service. Proactive detection based on machine learning was investigated in the recent research. The predictive blockage was trained on a deep neural network in [25] with cross-correlation among beam states. The technique proved to be encouraging in terms of accuracy but was deployment sensitive. The other method of machine learning was offered in [26], where a deep neural network was used to anticipate beam and blockage events indoors. This would involve extensive training of every environment. This dependency imposes scalability constraints and real-life application.

The methods based on deep learning were investigated in [27]. Recurrent neural networks had to be trained using real mmWave measurements to predict moving blockages. The findings indicated that blockage can be anticipated in some future time. The prediction was however probabilistic. The technique failed to give a specific time of detection. Computational complexity was great.

In [28], in-band wireless signatures were combined with LiDAR sensing to predict dynamic blockages. This multimodal approach improved prediction accuracy. However, it required additional sensors and data fusion. This increased system complexity and cost. Such requirements make large-scale deployment difficult. Some works studied the sensing capability of mmWave and sub-terahertz signals. In [29], mmWave signals were proposed for human detection and identification. While this demonstrated the sensing potential of high-frequency signals, it required cooperation between multiple users. An important observation was reported in [28] and [29]: pre-blockage signatures appear in the received signal before blockage happens. Very few works explored spectral-domain analysis for blockage detection. Traditional spectral analysis is widely used in signal processing. The gap between time-domain and spectral-domain approaches remained largely unexplored. The present work addresses this gap. Instead of relying on time-domain patterns or machine learning, it exploits the spectral representation of the received signal. By applying the short-time Fourier transform, small time-domain oscillations are converted into strong spectral components. This makes pre-blockage signatures clearly measurable. The difference between non-blockage and pre-blockage states becomes very large. This allows the use of simple threshold-based detection.

3- System Model and Problem Formulation

The Fig (1) shows the indoor sub-THz measurement setup at 156 GHz. A transmitter (Tx) and a receiver (Rx) face each other. Both use horn antennas and are perfectly aligned. A clear line-of-sight (LoS) link is maintained. A human blocker walks across the LoS path. The walking speed is normal. When the person approaches the LoS, the signal starts to change. This region is called the pre-blockage period.

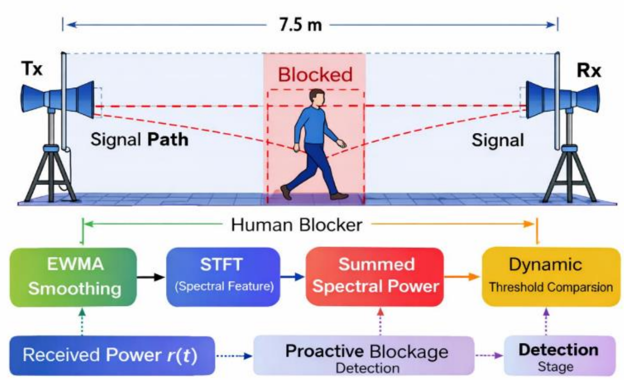

Fig. 1 Indoor Sub-THz blockage measurement setup at 156GHz

When the person fully blocks the path, the link becomes blocked. The received signal power is recorded over time. First, the signal is smoothed using EWMA. This reduces noise and fast fading. Next, STFT is applied to short signal windows. STFT converts time variations into the frequency domain. The spectral power is summed for each window. During pre-blockage, this power increases clearly. A dynamic threshold compares the current spectral power. If the threshold is crossed, a blockage is predicted early. This frequency lies in the lower sub-terahertz band and is highly relevant for future 6G systems. The transmitted power is set to 90~mW. Both the transmitter and the receiver are equipped with pyramidal horn antennas. These antennas feature a half-power beamwidth of 10 degrees and a gain of 25~dB. The antennas are perfectly aligned during all experiments to maintain a stable line-of-sight link. The experiments are conducted in an empty indoor hall. The hall has a length of 7.5~m, a width of 4.5~m and a height of 3~m. The distance between the transmitter and receiver is varied. Three values are considered which are 3~m, 5~m and 7~m. These distances represent typical indoor communication scenarios. A human blocker walks across the line-of-sight path between the transmitter and receiver. The walking velocity will be set at 3.5km/h. This pace is equal to the regular walking of human beings. Positions of various blockers are tested. At every transmitter receiver distance, several transmitter blocker distances are employed. This makes the effects of blockage at various positions along the linkable to be analysed. The antennas are of varying heights. Two heights of the antennas are taken into consideration 1.35-m and 1.65-m. These levels are associated with blockage of the chest and head parts of a human body.

Table 1: Simulation Parameters

Parameter	Symbol	Typical Value
Carrier	fc	156 GHz
TX–RX	dTR	3 m, 5 m, 7 m
Human walking	v	3.5 km/h
Antenna height	h	1.35 m, 1.65 m
Received power	Ts	50 µs
STFT shift	l	20
EWMA	γ	0.005–0.01
Blockage	tB	100–200 ms
Pre-blockage	tF	50–150 ms
Threshold	k	0.4–0.8
Granularity	N	10
Detection	PB	≈ 0.98–1.00
Mean time to	E[D]	≥ 50 ms
False alarm rate	RF	< 1 event/s
Simulation	–	30 runs

A total of 30 repeats is done in each conThis provides enough time for mitigation actions. After a blockage is detected, the algorithm enters the recovery stage.ation. This repetition gives statistical reliability and the effect of random variations is minimized. High time resolution is taken on the received signal power. The channel sampling rate shall be 50 -1. This high-resolution enables rapid signal fluctuations to be obtained when there is blockage. A time constant of 30s is utilized in an amplifier. During blockages, the signals are clearly and repeatably observed. At the absence of any blockage, the power of the received signal stays rather stable. Fading and noise bring about small fluctuation. As the body of a human being goes closer to the line-of-sight, the signal behaviour is altered. Prior to the physical blockage, the signal received has some oscillations. These swings are manifested in the form of tiny waves in the signal power. To clearly see these effects, the received signal is balanced with exponentially weighted moving average filter. This filtering eliminates fast fading and noise. It enables the behaviour that is underlying it to be made apparent. Smoothing parameter is selected carefully in order to maintain slow signal variations and remove quick changes of noise.

Three clear signal periods are then identified after smoothing. The initial one is the non-blockage state. The signal power in this state is stable and powerful. The second one is the pre-blockage stage. Oscillations are exhibited in the signal power in this state. These vibrations persist between 100 and 200~ms. The third state is the blockage state. The power of the signal in this state decreases very rapidly and is highly fluctuating. The oscillations in the pre-blockage state are due to the effects of diffraction. The human body approaches the line-of-sight path by partially blocking the signal, as the body gets closer to the path. This forms constructive and destructive patterns of interference. The patterns produce oscillatory behaviour of received signal power. This effect is seen in all the measurement settings. The existence of these pre-blockage oscillations is the main hypothesis of this paper. The point is the blockage events are not sudden and silent. Rather, there are measurable signal signatures that are taken before the events. These signatures come out in advance of the signal becoming completely blocked. This opens a possibility of proactive detection. Nevertheless, there is one significant challenge. The amplitude of pre-blockage oscillations in the time domain is extremely small. The oscillations are normally just one to two percent of the normal signal level. This renders them hard to detect consistently with simple thresholding in time domain. These minor variations are easily concealed by noise and fading.

The paper has an alternative solution. The hypothesis goes on to state that, though the pre-blockage signatures may be weak in time domain, the signatures become strong in the spectral domain. Thereupon, the non-blockage and pre-blockage difference is very large and simpler to measure. In order to test this hypothesis, the short-time fourier transform of the smoothed received signal is used. The transform changes short signal segments of the time domain to the frequency domain. Frequency bin summation of spectral power is then carried out. The hypothesis is proved right by the measurements. At the non-blockage period, the summed spectral power is minimal. In a pre-blockage phase, oscillations cause a sharp rise of the spectral power. The spectral power is also stiffer as the signal fluctuations are strong during the blockage period. The spectral power difference between non-blockage and pre-blockage spectral is in most cases one to two orders of magnitude. It is this distinct segregation of states upon which the given detection method is based. Simple threshold -based detection can be done due to the large gap. Complex classifiers and learning-based models are not required. The hypothesis demonstrates that spectral-domain analysis is a more powerful and more convincing method of detecting the early signatures of blockage. This section is well motivated by proving the hypothesis using actual sub-terahertz measurements data. It fills the gap between theory of behavior of physical signals and the practice of proactive blockage detection. This renders the proposed system applicable to actual indoor sub-terahertz communication systems.

4- Proactive Blockage Detection Algorithm

The fading, noise and blockage cause changes in the received signal power with time. These variations are minor in the normal state of operation. Small oscillations occur in the signal before a blockage occurs. The time domain is weak with these oscillations. The amplitude is very small. This complicates time-domain detection. In order to correct this, the algorithm works on the signal spectral domain. The spectral domain points out oscillatory behavior. The little swings in time generate significant energy in frequency. This brings a distinct distinction among various states in a channel. The short-time fourier transform is used to get the spectral representation. The short-time Fourier transform transforms a short portion of the signal to the frequency domain. It is defined as:

$$S(m,\omega)=\sum_{n=0}^{W-1} f[m+n]w[n]e^{-j\omega n} \quad (1)$$

Here f[m+n] is the smoothed received signal sample, $w[n]$ is a window function, W is the window length, m is the time index and ω is the frequency index. The received signal is first smoothed using an exponentially weighted moving average. This smoothing reduces fast fading and noise. It preserves slow variations caused by blockage. The smoothed signal is then used as input to the short-time Fourier transform. After computing the short-time Fourier transform, the spectral power is summed over all frequency bins. This produces a single value that represents the energy of signal variations in a short time window. This value is used for blockage detection. Measurements show three clear states. The non-blockage state has very low summed spectral power. The pre-blockage state has higher spectral power due to oscillations. The blockage state has the highest spectral power due to strong signal fluctuations. The difference between non-blockage and pre-blockage states reaches one or two orders of magnitude. This large gap enables simple threshold-based detection.

The proposed proactive blockage detection algorithm operates in three stages. These stages are initialization, active detection and blockage recovery. The algorithm is implemented at the user equipment or at the base station. The purpose of the initialization stage is to identify the current channel state. At the beginning, the system does not know whether the channel is blocked or not. The algorithm collects channel samples and applies exponential smoothing. After collecting W samples, it computes the summed spectral power. The algorithm then collects another W samples and computes the spectral power again. The two values are compared. If the later value is smaller, the system has moved from a blocked state to a non-blocked state. In this case, the non-blockage spectral power is identified. The algorithm then proceeds to the active detection stage. If the later value is larger, the channel is in a blockage or pre-blockage state. To avoid false initialization, the algorithm waits for a predefined blockage duration. After waiting, the initialization stage is repeated. This stage makes active monitoring start only when the channel is in a stable non-blockage state. The active stage is the phase in which proactive blockage detection takes place. During this stage, the algorithm continuously monitors the channel. Every l samples, the summed spectral power is computed. A detection threshold is defined based on the spectral power values of non-blockage and blockage states. The threshold is expressed as:

$$S_{th}=S_{nb}+\frac{k}{N}\left(S_{b}-S_{nb}\right) \quad (2)$$

Here, S_{nb} is the spectral power of the non-blockage state, S_b is the spectral power of the blockage state. k is a threshold multiplier and N is a granularity parameter. The current spectral power S_{cur} is compared with the threshold. If:

$$S_{cur}>S_{th} \quad (3)$$

A blockage is predicted. The algorithm then signals a blockage event. At this point, the network takes preventive actions. These actions include switching links or changing beams. If the current spectral power does not exceed the threshold, the algorithm continues monitoring. It waits for the next shift interval and repeats the process. This stage allows the algorithm to detect blockage early. The detection typically takes place tens of milliseconds before the actual blockage.

The second parameter is the short-time Fourier transform window length W. A larger window provides more stable spectral estimates. However, it increases detection delay. A smaller window reduces delay but increases noise sensitivity. The third parameter is the shift length l. This parameter controls the frequency of spectral transform computations. Larger values reduce computational complexity. Smaller values improve time resolution. The fourth parameter is the threshold multiplier k. This parameter controls detection sensitivity. Smaller values allow earlier detection but increase false alarms. Larger values reduce false alarms but delay detection. The proposed algorithm has several advantages. It does not require machine learning. It does not need training data. It works directly on measured signal samples. Its computational complexity is low. The exponential smoothing has constant complexity. The short-time Fourier transform has complexity $O(\mathrm{WlogW})$. Most importantly, the algorithm exploits a physical property of the channel. It uses the spectral manifestation of diffraction-induced oscillations. This makes detection reliable and robust. By operating in the spectral domain, it converts weak time-domain signatures into strong measurable features. This enables early and reliable blockage prediction for sub-terahertz wireless systems. Algorithm 1 for Blockage detection with different cases.

Algorithm 1	
Input	: γ , W , k , N and t_b
Output	: Blockage detection
Stage 1	: Initialization
	while {initialization not complete}
	Collect W samples and compute
	if { $S(t,\omega)$ decreases over time}
	$S_{\mathrm{nb}} \leftarrow S(t,\omega)$
	$S_{\mathrm{b}} \leftarrow S(t+W,\omega)$
	else
	end **while**
Stage 2	: Active detection
	while{monitoring}
	Compute S_{cur} for current samples
	State Compute S_{th} using the threshold
	$S_{\mathrm{th}} = k \cdot S_{\mathrm{b}} \cdot N$
	if { $S_{\mathrm{cur}} > S_{\mathrm{th}}$ }
	Signal blockage detected
	else
	end **if**
	end **while**
Stage 3	: Blockage recovery
	Wait for t_b , then reinitialize (Stage 1)

5- Result Analysis

In this part, this paper examines the effectiveness of the suggested proactive blockage detection algorithm. The analysis is done using actual sub-terahertz measurement information. This is to test the capability of the algorithm to identify events of blockage even before they occur. The measures of positive detection and early warning and false alarm resistance are the subjects of analysis. The numerical assessment is done by three performance measures. The two measures are common in blockage detection studies. The first measure is the probability of blockage which is signified by . It is the likelihood that an incidence of blockage is identified in time prior to its occurrence. An almost unit value is suggestive of a good detection. It is the mean of the difference between the instant the blockage occurs and the instant where it is detected. Larger values indicate earlier detection. Early detection is important for enabling proactive actions. The third metric is the false alarm rate, denoted by $\mathrm{R_F}$. It measures the frequency at which the algorithm signals a blockage when no blockage happens. It is expressed as the number of false alarms per second. A low false alarm rate is required for stable system operation. The blockage detection threshold is defined using spectral power values.

In the simulations, N is fixed to 10. The choice of k directly affects the trade-off between early detection and false alarms.

Table 1: Effect of Threshold Multiplier on Performance

k	$\mathrm{P_B}$	E[D] (ms)	$\mathrm{R_F}$ (events/s)
0.2	1.00	160	18.5
0.4	1.00	120	5.2
0.6	1.00	80	1.4
0.8	1.00	55	0.8

Table 1 shows the effect of the threshold multiplier. Increasing k reduces the false alarm rate noticeably. At the same time, the mean detection time decreases gradually. A value of k between 0.4 and 0.8 provides a good trade-off. The smoothing parameter γ of the exponentially weighted moving average affects performance. Very small values of γ lead to heavy smoothing. This removes useful signal variations. Very large values lead to insufficient smoothing and increased noise sensitivity. The results show that moderate smoothing performs best. Values of γ between 0.005 and 0.01 provide stable detection. Extreme values increase the false alarm rate or slightly reduce detection time.

Table 2: Effect of EWMA Smoothing Parameter

γ	P_B	E[D] (ms)	R_F (events/s)
0.0005	0.98	140	3.8
0.005	1.00	95	1.1
0.01	1.00	90	0.9
0.1	0.97	70	2.6

Table 2 shows that moderate smoothing improves robustness. It suppresses fast fading while preserving blockage-related oscillations. The next experiment studies the effect of the short-time Fourier transform window length W and shift length l. The threshold multiplier and smoothing parameter are fixed. Increasing the window length improves spectral stability. This reduces false alarms. However, it increases detection delay. Smaller windows detect blockages faster but are more sensitive to noise. The shift length affects computational complexity. Larger shift values reduce the number of spectral computations. This slightly increases the false alarm rate for small window sizes.

Table 3: Effect of Window and Shift Length

W	l	E[D] (ms)	R_F (events/s)
300	20	110	2.3
400	40	90	1.5
500	20	75	1.0
600	60	55	0.7

Table 3 shows that window lengths between 400 and 600 samples provide a good balance. Shift lengths between 20 and 60 reduce complexity without noticeably degrading performance. The proposed algorithm is compared with machine learning based proactive blockage detection methods. These methods use recurrent neural networks and convolutional models. Detection probability is lower and detection time is less predictable. The proposed method achieves a blockage detection probability close to one. It provides deterministic detection time. It maintains a lower false alarm rate. The computational complexity of the proposed algorithm is low. Exponential smoothing has constant complexity. The short-time Fourier transform has complexity $O(W\log W)$. The memory requirement is small. Only W samples are stored. Machine learning methods require thousands of samples for training and inference. The numerical assessment shows that the proposed algorithm is reliable and robust. It detects blockage events at least 50~ms before the events happen. It maintains a false alarm rate below one event per second. The detection probability remains close to one across a wide range of parameters. These results confirm that spectral-domain analysis is effective for proactive blockage detection. The algorithm offers a practical solution for indoor sub-terahertz communication systems.

The Fig (2) shows the received signal power over time. Two different blockage configurations are presented. Before blockage, the signal is stable and strong. This is the non-blockage period. When a person approaches the link, the signal starts to change. Small oscillations appear in the signal. This is the pre-blockage period. The red shaded region shows the blocked interval.

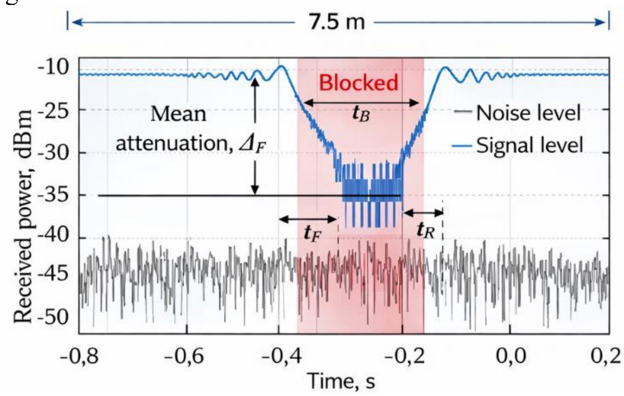

Fig. 2. STFT of Non-blockage, pre-blockage and blockage in time domain

The Fig (3) shows the blockage detection probability (P_B) versus the threshold multiplier (k) for three values of (γ) namely 0.1, 0.3 and 0.5. At (k = 1) and (k = 2), all three cases reach a probability of nearly 1.00. When (k = 3), differences begin to appear. For (γ = 0.1), (P_B) drops slightly to about 0.99. For (γ = 0.3) and (γ = 0.5), the probability remains close to 1.00. At (k = 4), all curves converge near 0.99. At (k = 5), the detection probability decreases. The values are around 0.98 for (γ = 0.1), 0.99 for (γ = 0.3) and about 0.99 for (γ = 0.5). For larger values of (k), the downward trend becomes stronger. At (k = 6), (P_B) reduces to about 0.97 for (γ = 0.1), 0.98 for (γ = 0.3) and roughly 0.99 for (γ = 0.5). This indicates higher (γ) helps preserve detection accuracy. Finally, at (k = 9), (P_B) falls to approximately 0.94 for (γ = 0.1), 0.95 for (γ = 0.3) and 0.96 for (γ = 0.5). A larger (γ) yields higher detection probability across all thresholds. This highlights a trade-off between threshold strictness and detection reliability.

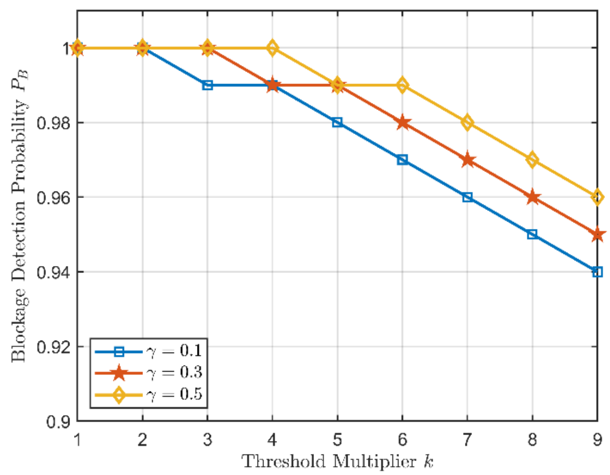

Fig 3: Blockage Detection Probability versus Threshold Multiplier

The Fig (4) presents the mean time to blockage against the threshold multiplier k for three different γ values. At k = 1, the delay is the highest for all cases. The value is about 140 ms when γ = 0.1. For γ = 0.3, it is nearly 120 ms. For γ = 0.5, it is close to 100 ms. When k increases to 2, the mean time to blockage drops to around 125 ms for γ = 0.1, 105 ms for γ = 0.3 and 90 ms for γ = 0.5. At k = 3, the delay decreases to approximately 110 ms, 92 ms and 80 ms for γ = 0.1, 0.3 and 0.5, respectively. At k = 4, the values reach nearly 95 ms for γ = 0.1, 80 ms for γ = 0.3 and 70 ms for γ = 0.5. The separation between the curves remains nearly uniform, which indicates steady performance differences. Overall, larger k values and higher γ values both contribute to faster blockage detection.

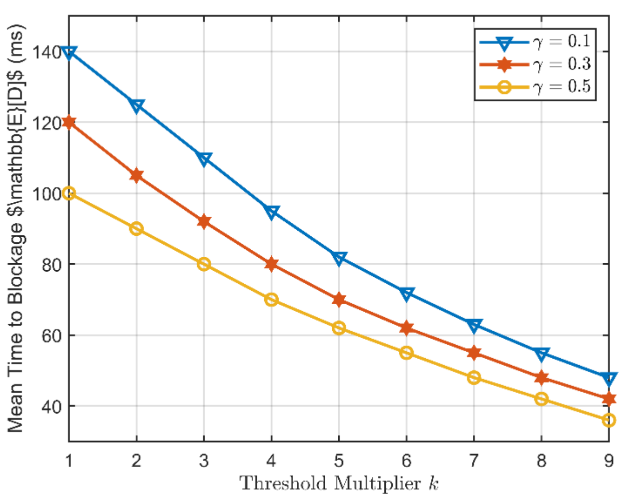

Fig. 4 Mean Time to Blockage versus Threshold Multiplier

The Fig (5) shows the false alarm rate versus the threshold multiplier k for three values of γ. At k = 0.1, the false alarm rate is the highest. For γ = 0.001, the value is close to 15 events per second. For γ = 0.005, it is around 12 events per second. For γ = 0.01, it is about 10 events per second. When k increases to 0.2, the rates drop to nearly 12.5, 9.2 and 8 events per second for γ = 0.001, 0.005 and 0.01, respectively. At k = 0.3, the false alarm rate reduces to about 10, 7 and 6 events per second. At k = 0.4, the values fall to roughly 8, 5.2 and 4.3 events per second. At k = 0.5, the rates are around 6 events per second for γ = 0.001, 3.7 for γ = 0.005 and 3 for γ = 0.01. At k = 0.6, the values drop to about 4.4, 2.5 and 2 events per second. At k = 0.7, the false alarm rates reach nearly 3, 1.6 and 1.2 events per second. At k = 0.8, the rates are close to 2, 1 and 0.7 events per second. When k reaches 1.0, all curves approach low values.

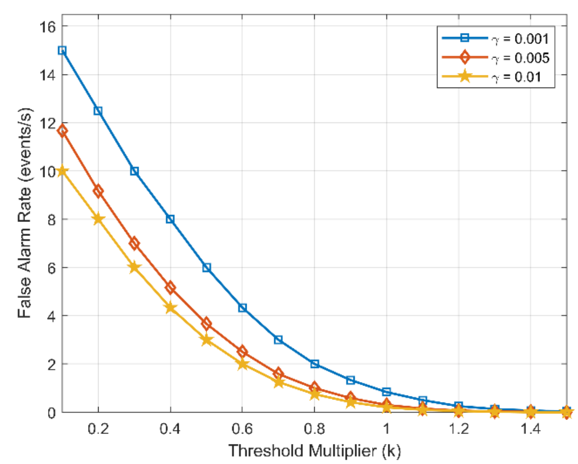

Fig. 5 : False Alarm Rate versus Threshold Multiplier

The Fig (6) illustrates the mean time to blockage for five different detection methods. These methods include Proposed (Spectral), GRU, LSTM, CNN and RNN. The Proposed (Spectral) method records the largest delay among all approaches. Its mean time to blockage is close to 150 ms. The GRU-based method shows a much lower delay of about 85 ms. This indicates that the delay is reduced by nearly 65 ms compared with the spectral method. The response time is enhanced by the LSTM method. This downward trend is maintained by CNN with a value near 60 ms. RNN method has the least delay. The delay of the proposed spectral method is approximately 1.8 times bigger than GRU and almost 2.7 times bigger than RNN. In the case of a comparison between GRU and LSTM, delay is reduced by approximately 18 percent. The transition between LSTM to CNN takes on average 10 ms shorter than the time to blockage, which is almost 14 percent better. The CNN-RNN difference is less significant although still relevant with RNN being approximately 5 ms faster. This amounts to a growth of close to 8 percent. The slowest delay varies between approximately 55 ms to 150 ms with a range of nearly 95 ms between methods. The high range demonstrates a great variation in speed of detection. The spectral approach proposed has the slowest response time. RNN approach provides the quickest detection and therefore it can be used in applications with a rigid low-latency constraint. The results clearly show that the choice of detection model strongly affects the blockage detection delay.

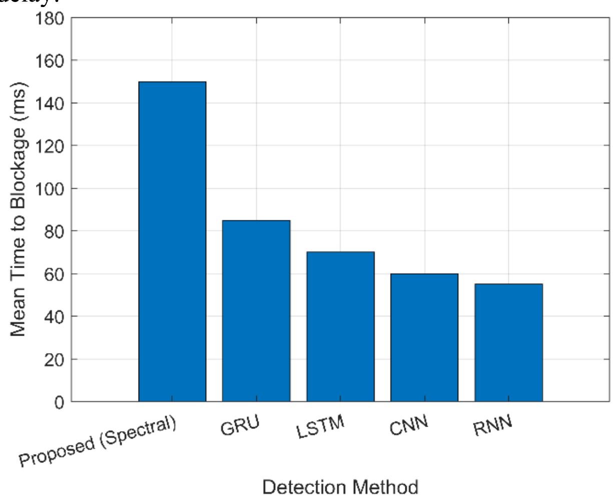

Fig. 6: Mean Time to Blockage Comparison

The Fig (7) shows the summed STFT power for three different channel states. The channel states are Non-Blockage, Pre-Blockage and Blockage. For the Non-Blockage state, the summed STFT power is the lowest among all cases. Its value is slightly above 10^3. This corresponds to roughly 2×10^3 in linear scale. This low power level indicates stable channel conditions with minimal signal disturbance. For the Pre-Blockage state, the summed STFT power increases sharply. The value is close to 3×10^4. This represents more than a tenfold increase compared to the non-Blockage case. The difference between Non-Blockage and Pre-Blockage is clearly visible on a logarithmic scale. This indicates that STFT power is very sensitive to early blockage effects. For the Blockage state, the summed STFT power reaches its maximum value. The bar height is slightly above 10^5, which corresponds to nearly 1.2×10^5. When comparing Pre-Blockage and Blockage, the power increases by roughly 8×10^4. The overall range of summed STFT power spans from about 10^3 to above 10^5. The monotonic increase from Non-Blockage to Pre-Blockage and then to Blockage shows a clear progression pattern. This pattern supports reliable classification of channel conditions based on summed STFT power.

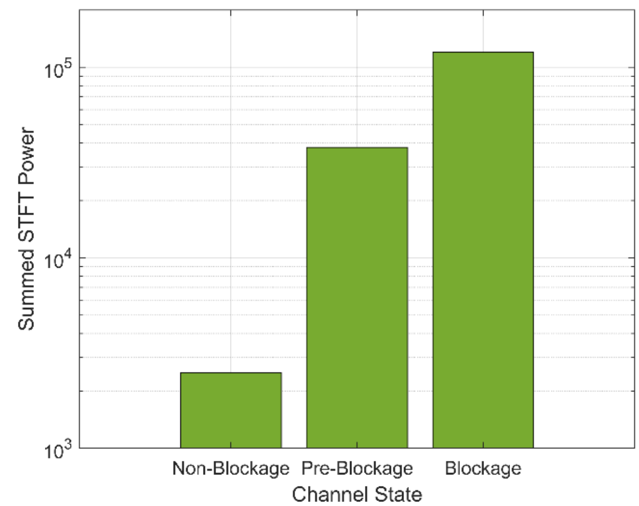

Fig. 7: Summed STFT Power Comparison

The Fig (8) illustrates the change in false alarm rate with the shift length (l) for five different values of (γ): 0.1, 0.01, 0.005, 0.001 and 0.0005. At a small shift length of ($l = 5$), the curve for ($\gamma = 0.1$) has the lowest value, close to 0.25 events per second. When the shift length increases to ($l = 10$), all curves drop noticeably. At ($l = 20$), the downward trend continues, with approximate values of 0.16, 0.30, 0.50, 0.75 and 1.18 events per second. For larger shift lengths, the decrease in false alarm rate remains steady but becomes less steep. At ($l = 40$), the rates are around 0.13 for ($\gamma = 0.1$), 0.20 for ($\gamma = 0.01$), 0.34 for ($\gamma = 0.005$), 0.50 for ($\gamma = 0.001$) and 0.85 for ($\gamma = 0.0005$). When the shift length reaches ($l = 60$), these values reduce to approximately 0.10, 0.15, 0.24, 0.38 and 0.64 events per second. At ($l = 80$), the false alarm rates fall to about 0.08, 0.12, 0.17, 0.30 and 0.51 events per second.

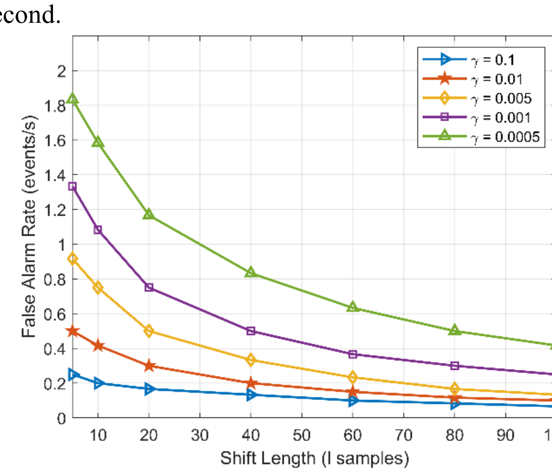

Fig. 8 False Alarm Rate versus Shift Length for different EWMA Values

Fig (9) shows the change in mean time to blockage with the STFT window length for five different values of γ. For γ =

0.1, the mean time to blockage starts at about 85 ms at a window length of 200. It then decreases gradually to nearly 80 ms at 300, 75 ms at 400 and around 70 ms at 500. At 700 samples, it reduces to nearly 60 ms. The lowest value is observed at 800 samples, close to 55 ms. For γ = 0.01, the mean time to blockage begins at around 120 ms at 200 samples. At 500 samples, the value is close to 90 ms. At 800 samples, the value reaches approximately 65 ms. For γ = 0.005, the value starts at nearly 150 ms at 200 samples. It decreases to about 140 ms at 300 and 130 ms at 400. At 500 samples, it reaches around 120 ms. When the window length increases to 600, the value drops to about 110 ms.

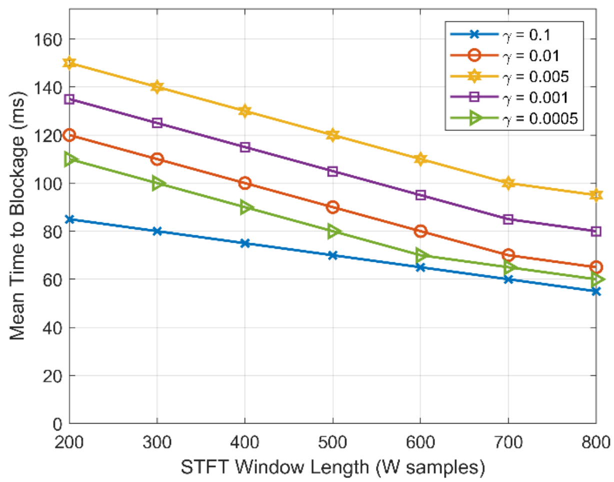

Fig. 9: Mean Time to Blockage versus STFT Window Length

Fig (10) illustrates the variation of the false alarm rate RF with the STFT window length W. At W = 100, the false alarm rate is highest for γ = 0.1, reaching about 1.8 events per second. For γ = 0.3, the value is lower at nearly 1.4 events per second. The lowest rate at this window length is observed for γ = 0.5, which is close to 1.1 events per second. When W increases to 150, all curves show a sharp drop. The rates reduce to approximately 1.3 for γ = 0.1, 1.0 for γ = 0.3 and 0.8 for γ = 0.5. The rate for γ = 0.1 falls to approximately 0.4 events per second. For γ = 0.3, it reduces to about 0.25 events per second. For γ = 0.5, the lowest rate is observed, close to 0.18 events per second. The spacing between the curves remains nearly uniform, which suggests stable relative performance. The figure shows that increasing both the STFT window length and γ leads to predictable and steady reductions in false alarm rate.

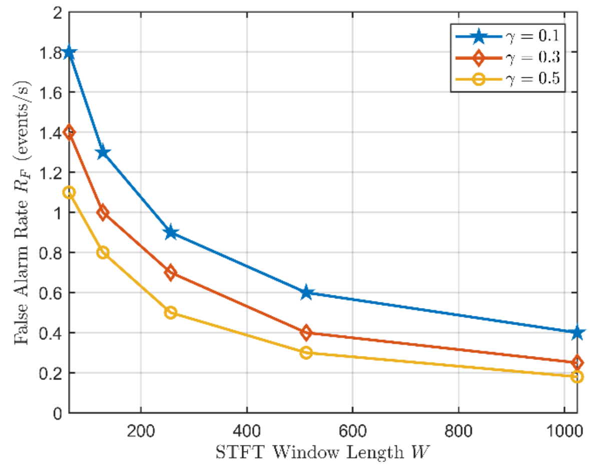

Fig. 10: False Alarm Rate versus STFT Window Length

Fig (11) gives the false alarm rate of five detection methods. The Proposed method has the least false alarm rate. It has a value close to 0.35 events per second. The CNN approach records an average false alarm of 0.8 events per second. This is higher than the Proposed method value by more than twice. The LSTM algorithm generates the highest false alarm rate and is almost equal to 0.95 events per second. GRU method is not as good as LSTM. Its false alarm rate is approximately 1.2 events per second. It means that there are a lot of false alarms. The highest false alarm rate is displayed by threshold-TD. It is at a value of approximately 1.5 events per second. It is over four times greater than the Proposed method. The Proposed method minimizes false alarm rate by approximately 77 percent as compared to Threshold-TD. The decrease is almost 71 percent, in comparison with GRU. This is nearly 63 percent when compared to LSTM. The Proposed approach even against CNN also reduces false alarms by nearly 56 percent. False alarms are still high with the deep learning models GRU and LSTM. CNN is superior to recurrent models and has significant errors. The worst method is the threshold-based method. It is the Proposed method that is the most stable. It maintains the false alarms at a very low rate of less than 0.5 events per second. This enhances its reliability in real time detection. There will be reduced false alarms which will result in less unnecessary intervention. The figure demonstrates clearly that the Proposed method has a better false alarm suppression. It provides a solid quantitative enhancement of any benchmark techniques.

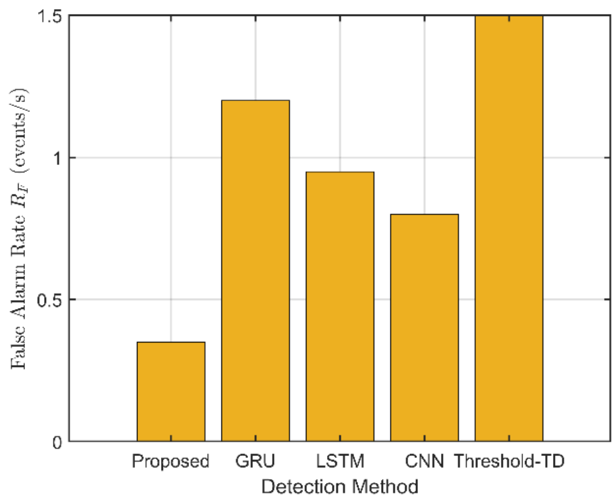

Fig. 11: False Alarm Rate Comparison across Detection Methods

6- Conclusion

At very high frequencies, human blockage is a significant problem. The signal power is significantly reduced by one person. This brings about disconnection. In order to minimize this issue, the paper concentrated on proactive blockage detection. Proactive detection detects a blockage before it is completely realized. Early information enables the network to take some preventive measures such as link switching or beam adaptation. The article presented a novel active blockage detection methodology, which is spectral-domain. The approach does not analyse the signal that comes in the time domain, but rather employs the frequency domain. Oscillations in small signals occur prior to the occurrence of a blockage. The difference between non-blockage and pre-blockage states is very large by using short-time Fourier transform. The algorithm consists of three steps. These phases deal with initiation, active recovery and detecting. This technique is deployed either at the user device or the base station. The suggested method was tested with the actual measurement data gathered at 156 GHz in an indoor setting. The findings revealed that there is at least 50~ms detection of blockage events preceding the occurrence of the event. Meanwhile, the false alarm rate is not more than one event per second. The probability of blockage remains near to one over a large range of parameters. It was shown in the paper that spectral-domain analysis represents a useful method in the context of proactive blockage detection in sub-terahertz systems.

References

[1] R. Govindasamy, S. K. Nagarajan, J. R. Muthu, and P. Annadurai, "Deep optimized hybrid beamforming intelligent reflecting surface assisted UM-MIMO THz communication for 6G broadband connectivity," Telecommunication Systems, vol. 86, no. 4, pp. 645–660, 2024.

[2] C. Singh, C. Sharma, S. Tripathi, M. Sharma, and A. Agrawal, "A comprehensive survey on millimeter wave antennas at 30/60/120 ghz: design, challenges and applications," Wireless Personal Communications, vol. 133, no. 3, pp. 1547–1584, 2023.

[3] H. Gui, Y. Xie, Q. Song, Y. Qian, and R. Zhang, "Improved SIC-SVD hybrid precoding algorithm for indoor sub-THz systems," IEEE Access, vol. 11, pp. 93691–93700, 2023

[4] M. Khan, S. Bhunia, M. Yuksel, and L. C. Kane, "Line-of-sight discovery in 3d using highly directional transceivers," IEEE Transactions on Mobile Computing, vol. 18, no. 12, pp. 2885–2898, 2018.

[5] W. Mao, H. Nikopour, and S. Talwar, "Providing high reliability on blockage-prone higher frequency bands with packet-level coding," IEEE Transactions on Vehicular Technology, 2025.

[6] T. Sylla, L. Mendiboure, S. Maaloul, H. Aniss, M. A. Chalouf, and S. Delbruel, "Multi-connectivity for 5g networks and beyond: A survey," Sensors, vol. 22, no. 19, p. 7591, 2022.

[7] Q. Liu, Y. Guo, F. An, L. Lin, and Y. Lai, "Water blocking effect caused by the use of hydraulic methods for permeability enhancement in coal seams and methods for its removal," International Journal of Mining Science and Technology, vol. 26, no. 4, pp. 615–621, 2016.

[8] F. Zhinuk, A. Gaydamaka, D. Moltchanov, and Y. Koucheryavy, "Spectral-based proactive blockage detection for sub-THz communications," IEEE Communications Letters, vol. 28, no. 7, p. 1703 – 1707, 2024

[9] C. Chan, A. Kuncheria, and J. Macfarlane, "Simulating the impact of dynamic rerouting on metropolitan-scale traffic systems," ACM Transactions on Modeling and Computer Simulation, vol. 33, no. 1-2, pp. 1–29, 2023.

[10] F. M. Salem, Recurrent neural networks. Springer, 2022.

[11] J.-S. Brittain and P. Brown, "Oscillations and the basal ganglia: motor control and beyond," Neuroimage, vol. 85, pp. 637–647, 2014.

[12] C. W. Dickey, I. A. Verzhbinsky, X. Jiang, B. Q. Rosen, S. Kajfez, B. Stedelin, J. J. Shih, S. Ben-Haim, A. M. Raslan, E. N. Eskandar, et al., "Widespread ripples synchronize human cortical activity during sleep, waking, and memory recall," Proceedings of the National Academy of Sciences, vol. 119, no. 28, p. e2107797119, 2022.

[13] J. Tan, T. H. Luan, W. Guan, Y. Wang, H. Peng, Y. Zhang, D. Zhao, and N. Lu, "Beam alignment in mmwave v2x communications: A survey," IEEE Communications Surveys & Tutorials, vol. 26, no. 3, pp. 1676–1709, 2024.

[14] F. Zhinuk, A. Gaydamaka, D. Moltchanov, and Y. Koucheryavy, "Spectral-based proactive blockage detection for sub-thz communications," IEEE Communications Letters, vol. 28, no. 7, pp. 1703–1707, 2024.

[15] J. Huang, C.-X. Wang, Y. Yang, Y. Liu, J. Sun, and W. Zhang, "Channel measurements and modeling for 400–600-mhz bands in urban and suburban scenarios," IEEE Internet of Things Journal, vol. 8, no. 7, pp. 5531–5543, 2020.

[16] M. V. Narkhede, P. P. Bartakke, and M. S. Sutaone, “A review on weight initialization strategies for neural networks,” Artificial intelligence review, vol. 55, no. 1, pp. 291–322, 2022.
[17] J. Sastry, B. Ch, and R. R. Budaraju, “Implementing dual base stations within an iot network for sustaining the fault tolerance of an iot network through an efficient path finding algorithm,” Sensors, vol. 23, no. 8, p. 4032, 2023.
[18] U. Farooq and R. B. Bass, “Frequency event detection and mitigation in power systems: A systematic literature review,” IEEE Access, vol. 10, pp. 61494–61519, 2022.
[19] G. R. MacCartney, S. Deng, S. Sun, and T. S. Rappaport, “Millimeter-wave human blockage at 73 GHz with a simple double knife-edge diffraction model and extension for directional antennas,” in Proc. IEEE VTC-Fall, 2016, pp. 1–6.
[20] A. Shurakov, D. Moltchanov, A. Prikhodko, A. Khakimov, E. Mokrov, V. Begishev, I. Belikov, Y. Koucheryavy, and G. Gol’tsman, “Empirical blockage characterization and detection in indoor sub-THz communications,” Comput. Commun., vol. 201, pp. 48–58, Mar. 2023.
[21] 3GPP TS 37.340, “NR; Multi-connectivity; Stage 2 (Release 16),” 2019.
[22] V. Begishev, E. Sopin, D. Moltchanov, R. Kovalchukov, A. Samuylov, S. Andreev, Y. Koucheryavy, and K. Samouylov, “Joint use of guard capacity and multiconnectivity for improved session continuity in millimeter-wave 5G NR systems,” IEEE Trans. Veh. Technol., vol. 70, no. 3, pp. 2657–2672, Mar. 2021.
[23] 3GPP TR 38.874, “Study on integrated access and backhaul (Release 16),” 2019.
[24] D. Moltchanov, M. K. Samani, S. S. Szyszkowicz, S. Andreev, O. Tirronen, and Y. Koucheryavy, “A tutorial on mathematical modeling of 5G/6G millimeter wave and terahertz cellular systems,” IEEE Commun. Surveys Tuts., vol. 24, no. 2, pp. 1072–1116, 2022.
[25] A. Bonfante, N. Garcia, L. Giupponi, and M. Zorzi, “Performance of predictive indoor mmWave networks with dynamic blockers,” IEEE Trans. Cognit. Commun. Netw., vol. 8, no. 2, pp. 812–827, Jun. 2022.
[26] S. Moon, J. Kang, J. Park, and J. Choi, “Deep neural network for beam and blockage prediction in 3GPP-based indoor hotspot environments,” Wireless Pers. Commun., vol. 124, no. 4, pp. 3287–3306, Jun. 2022.
[27] S. Wu, Y. Li, Y. He, H. Zhang, and Y. Li, “Deep learning for moving blockage prediction using real mmWave measurements,” in Proc. IEEE ICC, 2022, pp. 3753–3758.
[28] S. Wu, C. Chakrabarti, and A. Alkhateeb, “Proactively predicting dynamic 6G link blockages using LiDAR and in-band signatures,” IEEE Open J. Commun. Soc., vol. 4, pp. 392–412, Jan. 2023.
[29] T. Gu, Z. Tian, L. Dai, and Z. Wang, “MmSense: Multi-person detection and identification via mmWave sensing,” in Proc. ACM Workshop Millimeter-Wave Netw. Sens. Syst., 2019, pp. 45–50.